Nonlinear Penetration of Whistler Pulses into Collisional Plasmas via Conductivity Modifications

J. M. Urrutia and R. L. Stenzel
Department of Physics, University of California, Los Angeles, California 90024-154705
(Received 23 May 1991)

A strong electromagnetic impulse ($\Delta t \simeq 0.2$ μs) with central frequency in the whistler-wave regime is applied to a large laboratory plasma dominated by Coulomb collisions ($\nu_{ei} \simeq \omega \ll \omega_{ce} \ll \omega_{pe}$). Local electron heating at the antenna and transport along $\mathbf{B}_0$ create a channel of high conductivity along which the whistler pulse penetrates with little damping. Because of its rapid temporal evolution, this new form of modulational instability does not involve ducting by density gradients which require ion time scales to develop.

PACS numbers: 52.35.Mw, 52.35.Hr, 52.40.Fd, 52.50.Gj

Nonlinear effects due to strong electromagnetic fields are of general interest in plasma physics, particularly in laser-plasma interactions [1], rf heating [2], and active space experiments [3]. In magnetized plasmas, filamentation of antenna-launched whistler waves has received considerable attention [4–6]. Thermal filamentation has been considered [7–9] whereby the electron heating is mainly caused by the antenna near-zone fields. It is generally accepted that the ducting of whistlers [10] in thermal filaments is caused by density gradients rather than temperature gradients. In the present Letter we report new observations of preferred wave propagation in a thermal filament *without* density gradients. Such transient filaments are created with an intense electromagnetic impulse (half cycle) which heats electrons so rapidly that pressure equilibration has not taken place. Also, density variations by ionization and ponderomotive force effects are negligible. On the time scale of the parallel electron heat flow, the wave penetrates into the collisional plasma because a high-conductivity filament capable of supporting the wave packet is formed. This new form of a "modulational instability" does not guide the wave by refraction but by a modulation of the conductivity in a uniform but collisional magnetoplasma.

The experiment is performed in the afterflow of a large, pulsed dc discharge with parameters indicated in Fig. 1(a). A short current pulse ($\Delta t = 0.2$ μs, 10 kV, 250 A) is applied to a two-turn, 4.5-cm-diam insulated magnetic loop antenna with its surface normal along $\mathbf{B}_0$. The peak applied energy density far exceeds the particle energy density ($B_{\max}^2/2\mu_0 \simeq 10^4 nkT$). With a vector magnetic probe movable in three dimensions, the time-varying magnetic field $\mathbf{B}(\mathbf{r},t)$ is measured from repeated experiments. Plasma parameters are obtained from a movable Langmuir probe. Its characteristic is obtained by measuring the current versus time at fixed voltage which is incremented after several repeated pulses.

While the properties of plane whistler waves are well known [10], the field topology of a single pulse bounded in space and time is less familiar. Figure 1(b) indicates a snapshot of the field components of such a whistler oscillation in a collisionless background plasma. A contour plot in the y-z plane shows a longitudinal B_z component which is not found in plane whistler waves. The transverse field components (B_x,B_y) are projected as field lines onto an x-y plane at $z = 30$ cm. The spiraling field can be decomposed into two opposing toroidal fields, each linked

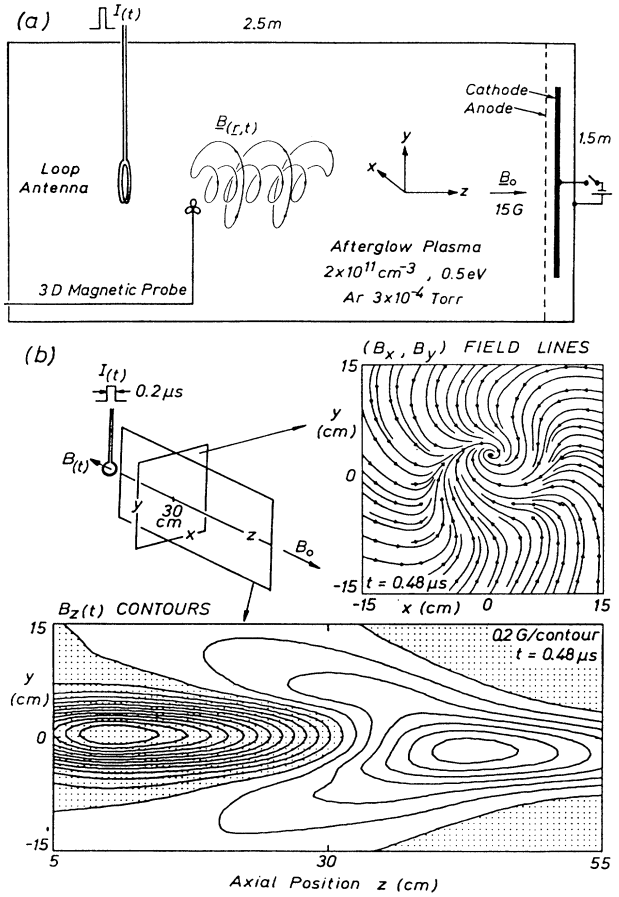

FIG. 1. (a) Experimental setup and typical plasma parameters. (b) Magnetic field components of a whistler pulse displayed at a fixed time in two orthogonal planes. The resultant field lines form short nested flux ropes as sketched in (a). (Shaded areas, $B_z < 0$; white areas, $B_z > 0$.)

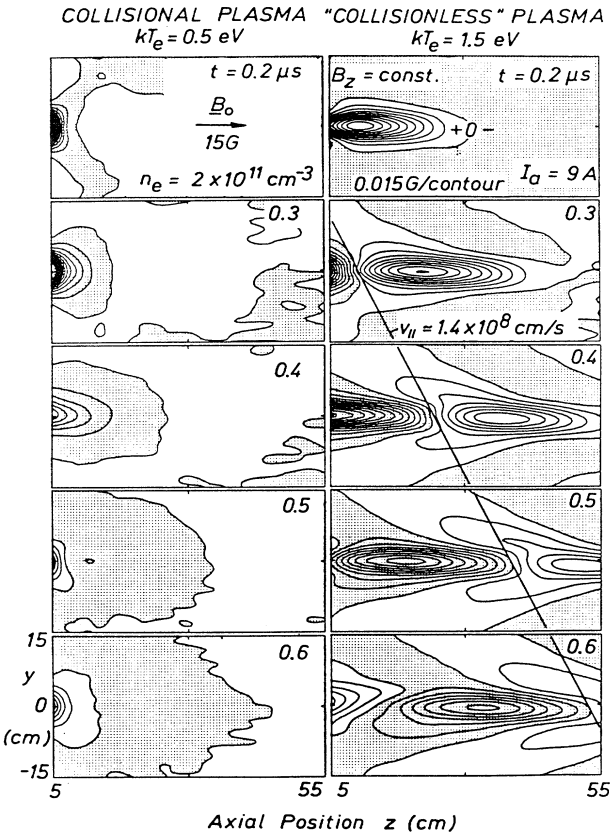

FIG. 2. Propagation of a small-amplitude whistler pulse in a cold collisional plasma (left) and in a heated "collisionless" plasma (right). A wave is excited in the latter but is damped in the former ($\nu_{ei} > \omega$). (Shaded areas, $B_z < 0$.)

with the axial solenoidal $\pm B_z$ field, and resulting in a flux-rope-like helical topology in three dimensions. Each helical field line near the axis closes via an outer return helix as sketched in Fig. 1(a). Such field topologies also evolve self-consistently from short current pulses to electrodes [11] where they have been shown to form force-free electromagnetic fields ($\mathbf{J}\times\mathbf{B}+\rho\mathbf{E}=0$) [12].

The propagation of small-amplitude whistler pulses is shown in Fig. 2 in both a cold collisional ($\nu_{ei} > \omega$) afterflow plasma and a heated "collisionless" ($\nu_{ei} < \omega$) plasma. Contours of constant $B_z(t)$ are shown in the y-z plane at different times t after applying the current pulse to the loop antenna. While in the collisionless plasma a well-defined wave detaches from the antenna, the wave is strongly damped in the collisional plasma and significant fields exist only in the near-zone of the antenna.

The nonlinear penetration of large-amplitude whistler pulses into a collisional plasma is demonstrated in Fig. 3. Displayed are contours of constant wave magnetic field, $(B_x^2+B_y^2+B_z^2)^{1/2}=$const, in y-z planes at different times t and for different antenna currents I_a. For small antenna currents ($I_a \simeq 10$ A), no wave leaves the antenna, but at larger currents ($I_a = 50$ A) a damped wavelet detaches, and finally, at $I_a = 250$ A, a wave packet propagates along $\mathbf{B}_0$ essentially as in a collisionless plasma. It is evident that at large amplitudes the plasma properties have been changed.

Figure 4 presents evidence for strong electron heating from observations of visible light detected with a photomultiplier tube ensemble averaging over many repeated events. The antenna current (top trace) produces light pulses (bottom traces) which propagate axially and are

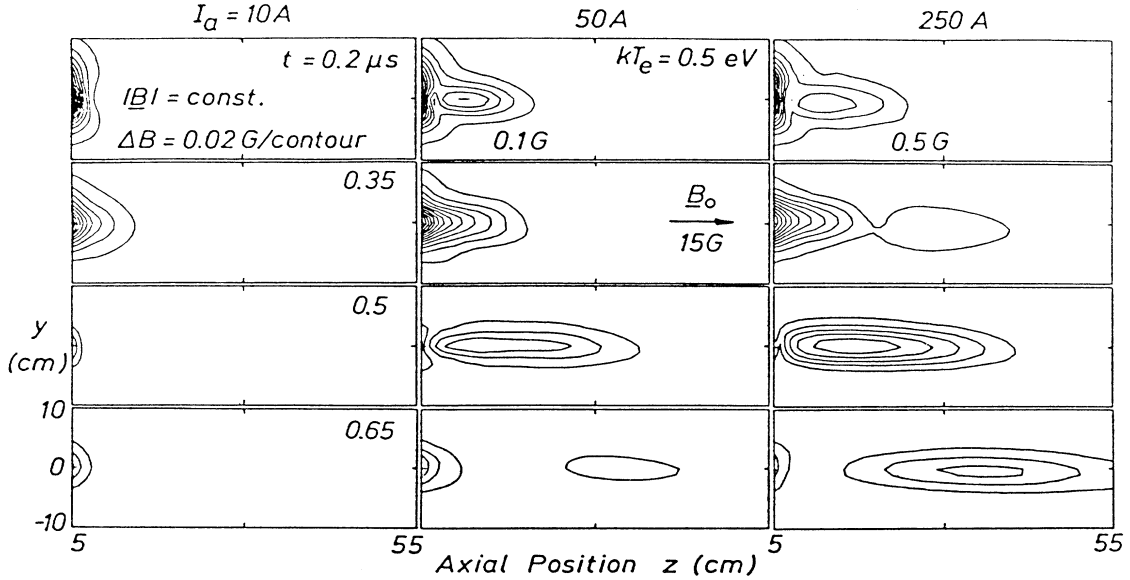

FIG. 3. Nonlinear wave penetration into a uniform collisional plasma. Contours of constant wave magnetic field in y-z planes at different times t and different antenna currents I_a. At small currents ($I_a \leq 10$ A) no wave is excited; at large currents ($I_a > 50$ A) a wave detaches and propagates along $\mathbf{B}_0$.

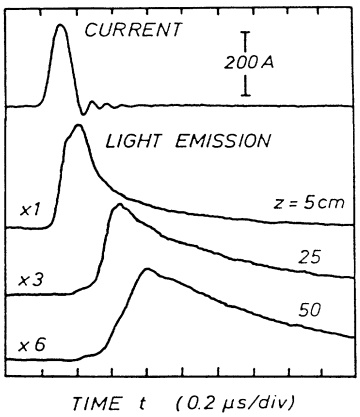

FIG. 4. Evidence of strong electron heating by the antenna current pulse (top trace) through visible light emission observed at different axial distances z from the antenna (bottom traces).

confined radially to the flux tube of the antenna.

Detailed *in situ* measurements of the plasma parameters have been performed with probes and are summarized in Fig. 5. Typical probe characteristics ($\log I$ vs V) at a fixed time t for different axial distances z from the antenna are shown in Fig. 5(a). Far from the antenna the temperature is unperturbed (0.5 eV), while nearby the electrons have been strongly heated ($kT_e \simeq 11.5$ eV). At intermediate distances non-Maxwellian tails are observed which may arise from the velocity dispersion of the expanding hot electrons near the source. Axial profiles of the bulk electron temperature at different times after the heating pulse are shown in Fig. 5(b). Electron heating starts near the antenna and expands along $\mathbf{B}_0$ at a speed $v_\parallel \simeq (30\ \text{cm})/(0.2\ \mu\text{s}) \simeq 1.5\times 10^8$ cm/s comparable to the wave speed ($v_\parallel \simeq 1.4\times 10^8$ cm/s). The heat transport is thought to be diffusive since space-charge fields prevent electron losses in the heated region ($n_i \simeq n_e \simeq$ const). After the rapid heating and axial transport, the electron temperature decays slowly (see inset), due to axial end losses and weak cross-field transport. The radial profiles of electron temperature and density at $r=0$, $z=25$ cm, and $t=1$ μs are shown in Fig. 5(c). While the temperature varies radially by an order of magnitude, the density is still uniform to within measurement accuracy ($\pm 10\%$). Thus, during the earlier propagation of the wave ($t < 1$ μs), ducting by density gradients cannot be the cause for the wave to follow the heated flux tube. The inset to Fig. 5(c) shows the scaling of the electron temperature with antenna current. For $I_a < 10$ A the plasma perturbations are negligible; for $I_a \simeq 250$ A the strong antenna field ($B_{\max} = \mu_0 N I_a / 2 r_a \simeq 140\ \text{G} \gg B_0$) and, to a lesser degree, the wave field ($B_{\text{wave}} \simeq 2$ G) cause strong electron heating ($T_{e,\max}/T_{e,0} \simeq 20$).

The physical mechanism by which the nonlinear wave penetrates into the collisional plasma is thought to be the generation of a hot plasma channel whose conductivity

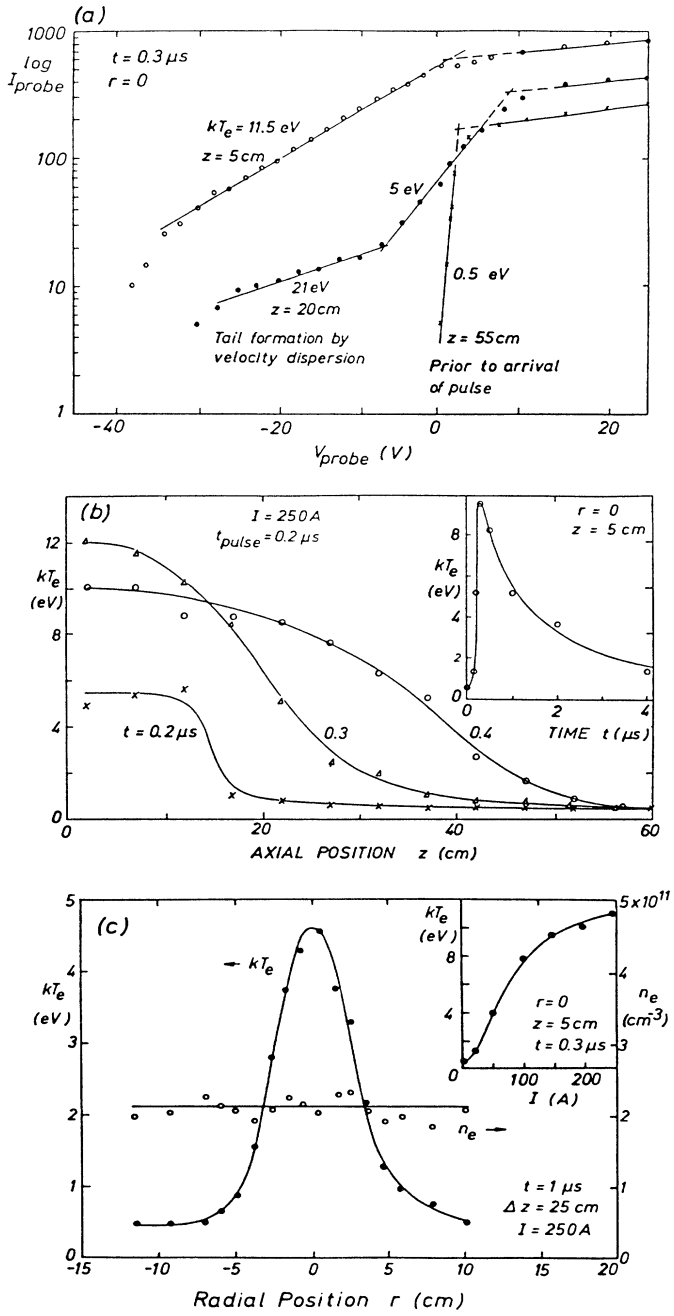

FIG. 5. Time- and space-resolved probe measurements of plasma parameters. (a) Langmuir probe traces sampled at a fixed time on axis at different distances from the antenna indicating strong axial temperature variations. (b) Axial temperature profiles at different times indicating parallel heat flow away from the antenna. (Inset: Slow temperature relaxation after rapid initial heating.) (c) Radial profiles of density and electron temperature at a time ($t=1$ μs) when the wave packet has passed. Note that the density profile is still uniform while the temperature in the antenna's flux tube is an order of magnitude higher than in the surrounding plasma. (Inset: Increase of kT_e with antenna current I_a near the antenna shortly after pulse application.)

($\sigma \propto T_e^{3/2}$) is 1–2 orders of magnitude larger than that of the surrounding cold plasma. The high-conductivity channel enables the wave packet to flow along $\mathbf{B}_0$ with little damping. If the parallel heat flow is slower than the wave (Fig. 3, $I_a = 50$ A), the latter will be damped when leaving the front of the heated channel. If, as in the present pulsed experiment, the energy input is finite ($I_a V_a \Delta t \simeq 250$ A $\times$ 10 kV $\times$ 0.2 μs = 0.5 J), the temperature will decay and the penetration length will be limited.

The present observation of nonlinear wave penetration is not only restricted to antenna-launched whistlers but also to pulsed currents applied with electrodes. These have been observed to penetrate along $\mathbf{B}_0$ at large amplitudes while spreading across $\mathbf{B}_0$ at small amplitudes [13]. Such transient currents are transported by whistlers [14]. The observations may also be relevant to the nonlinear properties of current filaments in plasmas described by Salingaros [15].

The authors gratefully acknowledge support of this work from Grants NSF No. PHY87-13829, No. ATM90-12709, and NASA No. NAGW-1570.

[1] R. D. Jones *et al.*, in *Laser Interaction,* edited by H. Horna and G. H. Miley (Plenum, New York, 1988), Vol. 8, p. 221.
[2] V. E. Golant and V. I. Fedorov, *rf Plasma Heating in Toroidal Fusion Devices* (Consultants Bureau, New York, 1989).
[3] B. Thidé, Phys. Scr. **T30**, 170 (1990).
[4] R. Stenzel, Phys. Fluids **19**, 865 (1976).
[5] H. Sugai *et al.*, Phys. Fluids **21**, 690 (1978).
[6] G. Yu Golubyatinikov *et al.*, Zh. Eksp. Teor. Fiz. **96**, 2009 (1989) [Sov. Phys. JETP **69**, 1134 (1989)].
[7] H. Washimi, J. Phys. Soc. Jpn. **34**, 1373 (1973).
[8] V. I Karpman *et al.*, J. Plasma Phys. **31**, 209 (1989).
[9] A. G. Litvak, Zh. Eksp. Teor. Fiz. **57**, 629 (1969) [Sov. Phys. JETP **30**, 344 (1970)].
[10] R. A. Helliwell, *Whistlers and Related Ionospheric Phenomena* (Stanford Univ. Press, Stanford, 1965), Chap. 3.
[11] R. L. Stenzel and J. M. Urrutia, Phys. Rev. Lett. **65**, 2011 (1990).
[12] V. A. Osherovich and E. B. Gliner, Sol. Phys. **117**, 391 (1988).
[13] J. Coroneus *et al.*, EOS Trans. Am. Geophys. Union **70**, 1285 (1989).
[14] R. L. Stenzel and J. M. Urrutia, J. Geophys. Res. **95**, 6209 (1990).
[15] N. A. Salingaros, Phys. Scr. **43**, 416 (1991).